Thermal–mechanical study of functionally graded dental implants with the finite element method

F. Wang,[1] H.P. Lee,[1,2] C. Lu[1]
[1]*Institute of High Performance Computing, 1 Science Park Road, No 01-01 The Capricorn, Singapore Science Park II, Singapore 117528, Singapore*
[2]*Department of Mechanical Engineering, National University of Singapore, 9 Engineering Drive 1, Singapore 117576, Singapore*

Received 23 June 2005; revised 21 March 2006; accepted 22 March 2006
Published online 25 September 2006 in Wiley InterScience (www.interscience.wiley.com). DOI: 10.1002/jbm.a.30855

Abstract: This article investigates the thermal–mechanical performance of hydroxyapatite/titanium (HA/Ti) functionally graded (FG) dental implants with the three-dimensional finite element method. The stresses induced by occlusal force for the present HA/Ti FG implant are calculated to compare with the corresponding stresses for the titanium dental implant. Thermal–mechanical effect of temperature variation due to daily oral activity is also studied. The HA/Ti FG dental implant performance is evaluated against the maximum von Mises stress, which is the general performance indicator, the first principal/tensile stress for mechanical failure of implant-bone-bond and the third principal/compressive stress for bone absorption. Simulation results indicate that under the influence of occlusal force only, the FG implants with different HA fraction along the implant length perform almost equally well, while the titanium implant sustains much higher von Mises stress. However, when thermal stress is also considered, the FG implant having HA fraction exponential index of $m = 2$ with temperature decrease of 20°C yields the highest first principal and von Mises stresses among all the FG and titanium implants. © 2006 Wiley Periodicals, Inc. J Biomed Mater Res 80A: 146–158, 2007

Key words: thermal–mechanical study; finite element simulation; hydroxyapatite/titanium functionally graded dental implant; fraction exponential rule

INTRODUCTION

Dental implant is a very popular clinical surgery to restore the functionality of decayed teeth. Many requirements such as the biocompatibility, mechanical suitability, thermal conductivity, etc. have to be satisfied. Biocompatibility is one of the major concerns for a dental implant surgery. It refers to the manner as to how the biological environment reacts to the presence of the implant, which is alien to the biological environment and could be hazardous or destructive. On the other hand, some materials have very positive effect on the biological environment,[1] such as the bioceramics, especially calcium hydroxide, which are bioactive to approach the nature of the natural biomaterials. In pursuit of high biocompatibility while maintaining the mechanical suitability, the bioceramic is very often used to coat the metal implant. Studies on the coated implant-bone-bond strength have been reported.[2–5] Although enhancements have been observed in the biocompatibility and the implant-bone-bond strength, the interface of the bioceramic with the metal may be another source of thermal–mechanical failure.[5]

In view of the fact that natural biomaterials are actually functionally graded, bioceramic/metal, to be specific the hydroxyapatite/titanium (HA/Ti) functionally graded (FG) dental implant is regarded as the most promising replacement for the lost dentin. Watari et al.[6] fabricated the HA/Ti FG dental implant and tested its biocompatibility in Wistar strain rat. They observed that HA/Ti FG dental implant had better biocompatibility than Ti implant. Yokoyama et al.[7] investigated the mechanical properties and biocompatibility of HA/Ti FG implant fabricated by spark sintering method and reported that much improvement was achieved by this method. Chu et al.[8] tested the bending strength of HA/Ti FG implant-bone-bond to be 159 MPa. Zhu et al.[9] tested the bonding shear strength of HA/Ti FG implant to be 6.49 MPa after implanted for 3 months. Chu et al.[10] designed optimally and fabricated HA/Ti FG material, based on the criterion of

Correspondence to: F. Wang; e-mail: wangf@ihpc.a-star.edu.sg

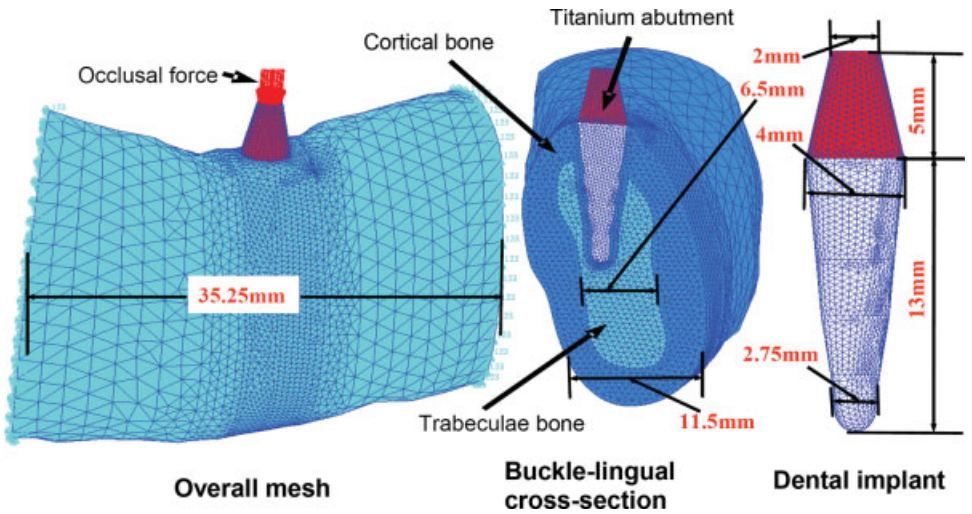

Figure 1. Overall mesh with the boundary and loading conditions. [Color figure can be viewed in the online issue, which is available at www.interscience.wiley.com.]

minimum residual thermal stress. Hedia and Mahmoud[11] used the finite element (FE) method to optimize the HA/Ti FG dental implant, based on the criterion of minimum von Mises stress.

In the present study, the three-dimensional FE method is adopted to study the HA/Ti FG dental implant performance with reference to the peri-implant stresses. The commercial titanium dental implant of Bioform® system is replaced by HA/Ti FG material. Since the higher peri-implant tensile stress would imply higher likelihood of implant-bone-bond failure and compressive stress would cause the bone absorption, the mechanical performance of implant is evaluated with reference to the peri-implant first principal/tensile and the third principal/compressive stresses, in addition to the general performance indicator of von Mises stress. Parametric studies on different mixture of the FG dental implant following the Takashi and Naotake's[12] exponential law is implemented.

On the other hand, the process of swallowing hot/cold food or water causes temperature change in the oral environment. The temperature variation could be as high as 20°C.[13] The current study also evaluates the thermal–mechanical effect of temperature change on the FG dental implant performance.

TABLE I
Material Properties

Material	Young's Modulus (MPa)	Poisson's Ratio	CTE (K^{-1})
Titanium	115,000	0.33	1.19×10^{-5}
Hydroxyapatite	11,000	0.3	1.6×10^{-5}
Trabecular bone	1,370	0.3	1.0×10^{-5}
Cortical bone	13,700	0.3	1.0×10^{-5}

THE FE MODEL

The geometry of implant for the first lower molar and the mandible is obtained from the FE model of Las Casas et al.,[14] which is built from a computerized tomography scan of a dental implant of Bioform® system and the CT scan of a mandible. The implant is 13-mm long and 4-mm in diameter. It is tapered with the oblique surfaces parallel to the mesial–distal section. A layer of cortical bone of 1-mm thick is assumed to form around the implant.[14] In the present study, only the dental implant and

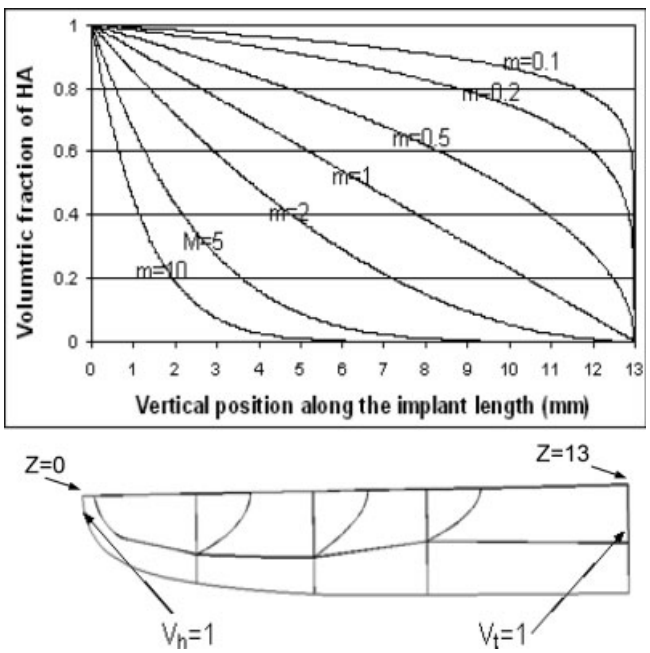

Figure 2. Volumetric fraction of hydroxyapatite along the length of implant.

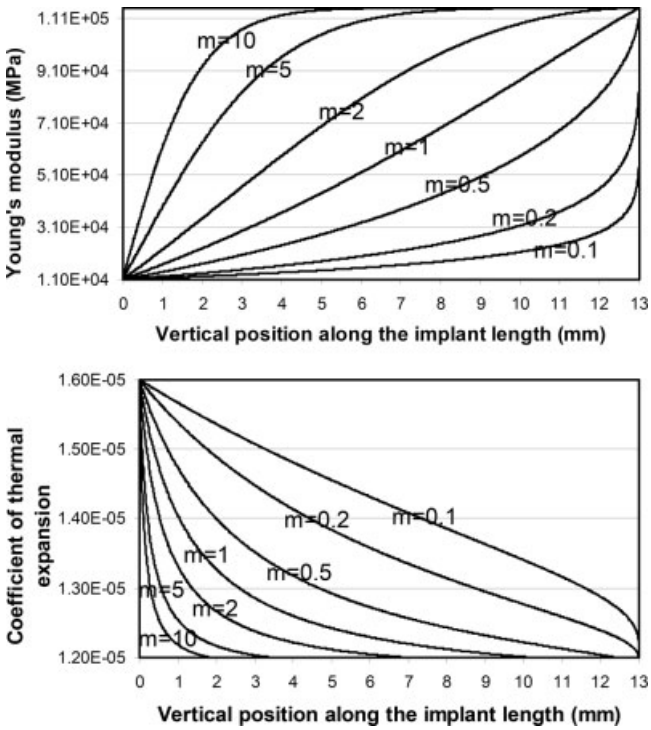

Figure 3. Variations of Young's modulus and CTE along the length of implant.

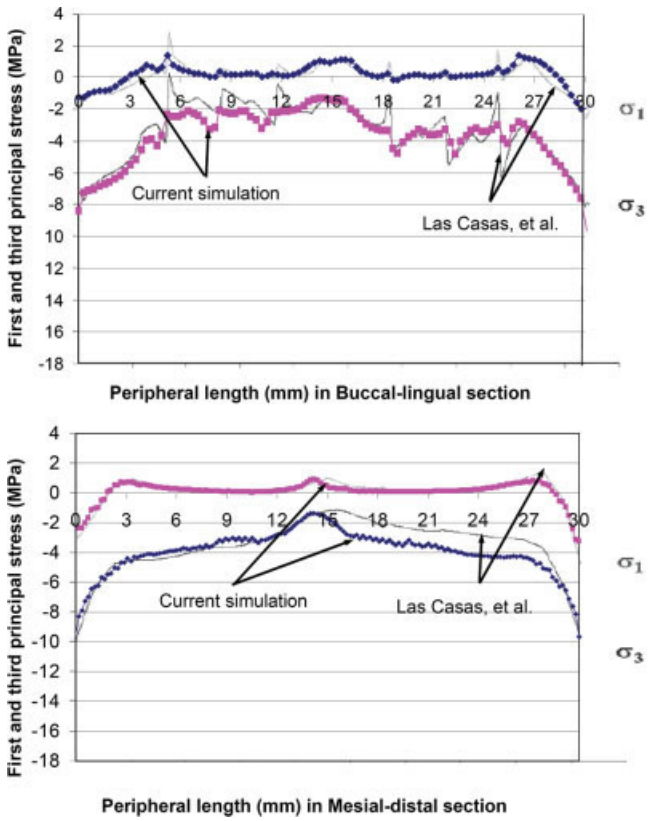

Figure 5. Verification of current model against results by Las Casas et al.[14] [Color figure can be viewed in the online issue, which is available at www.interscience.wiley.com.]

the immediate surrounding stomatognathic system is modeled. The surrounding bone tissue is large enough to maintain similar local stress distribution around the dental implant as that with a full mandible. The material for the abutment is titanium, while HA/Ti FG material is used for the implant.

The FE mesh with boundary and loading conditions is presented in Figure 1. The dimensions for the mandibular segment and the implant are indicated in this figure. The two end surfaces are fully restricted from any movement. A fully bonded interface is assumed between the implant and the surrounding bone tissue so that they share the same nodes at the contacting interfaces.

The occlusal force varies from person to person and also from time to time for a specific person. The estimated range of the force in a complete dentition is about 20–200*N*.[14] In the present study, the authors aim to compare the relative thermal–mechanical per-

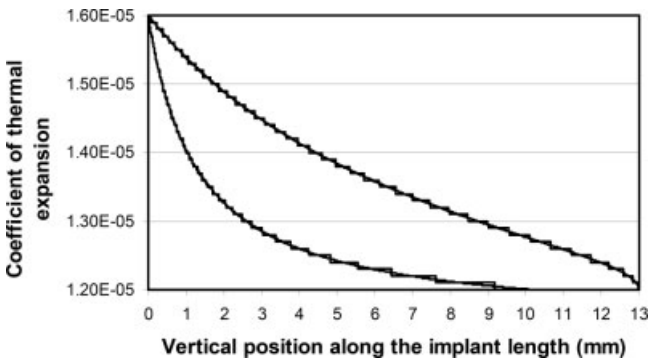

Figure 4. Line segment approach to the variation of CTE.

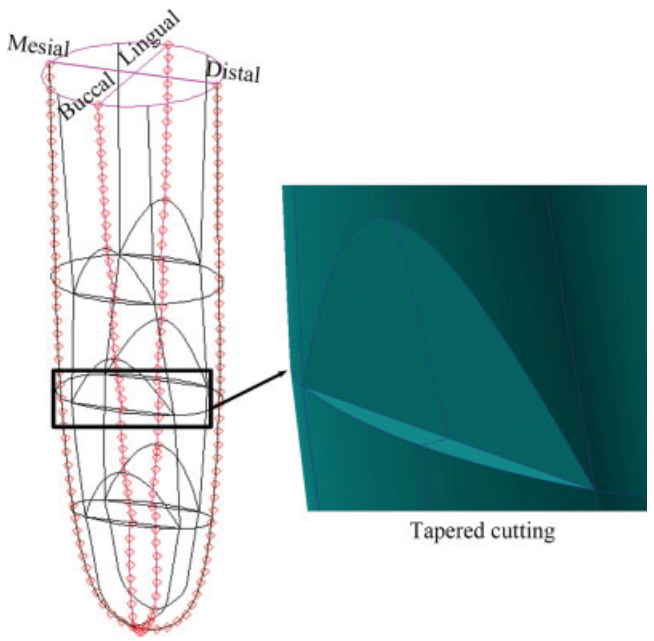

Figure 6. Peripheral nodes for presentation of the stress. [Color figure can be viewed in the online issue, which is available at www.interscience.wiley.com.]

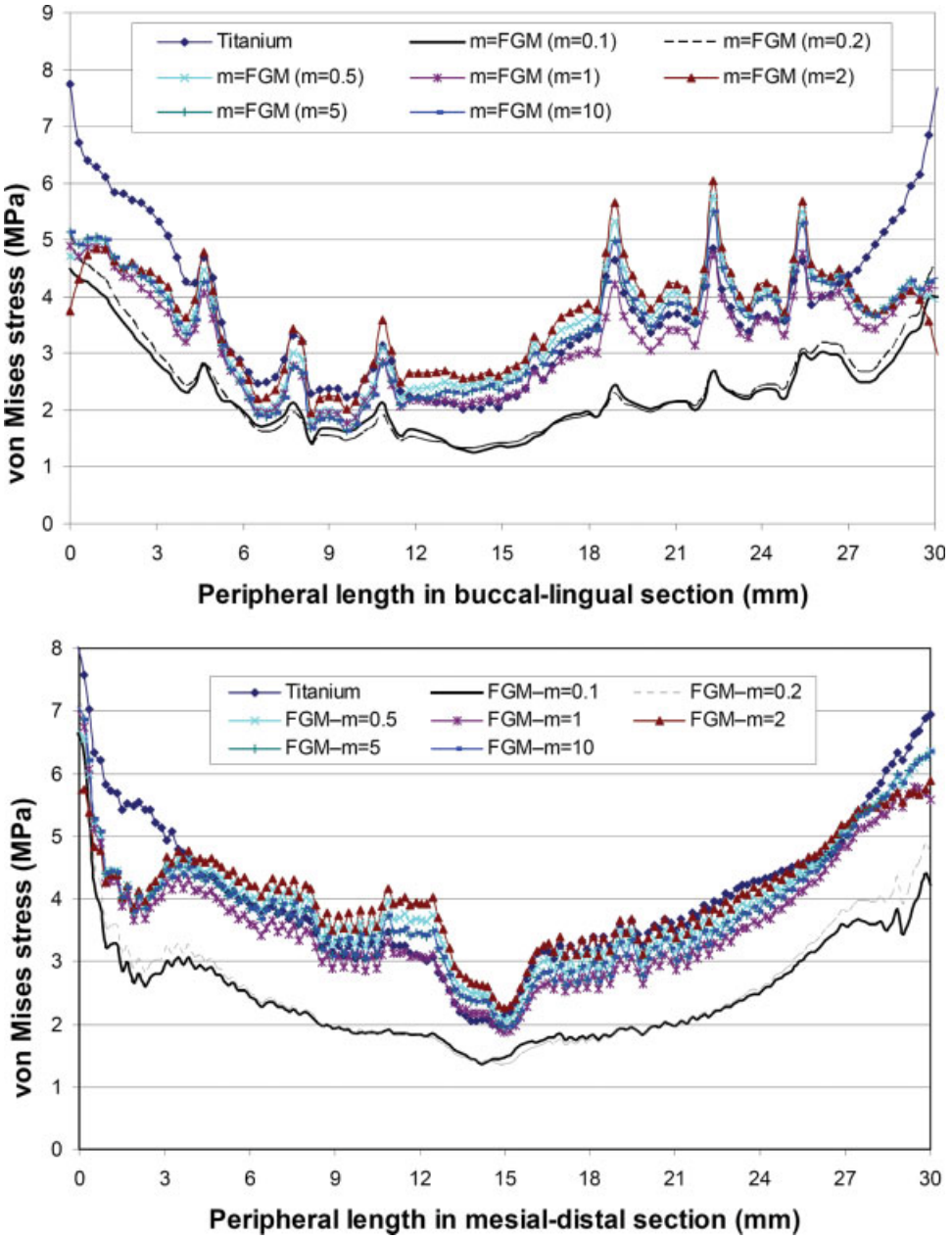

Figure 7. Peri-implant von Mises stress under occlusal force only. [Color figure can be viewed in the online issue, which is available at www.interscience.wiley.com.]

formance of FG dental implant with different fraction of composition along the length of the implant instead of deriving the exact stress level during the dentition. Thus, a 100*N* vertical force, which represents an average occlusal force, is applied as a uniform pressure on the top surface of the abutment (Fig. 1).

On the other hand, according to Toparli and Sasaki,[13] oral temperature increase or decrease caused by daily activity, such as swallowing hot or cool water, can be as high as 20°C. Thermal stress is then calculated through temperature load, which is assigned −20°C and 20°C for the whole stomatognathic system.

The properties for each material are tabulated in Table I.[13,14] It should be mentioned that for the CTE of bones very different values were given by different researchers, e.g., 0.01×10^{-6} K^{-1} was reported by Ahmed et al.[15] and 27.5×10^{-6} K^{-1} by Duck et al.[16] On the other hand, Toparli and Sasaki used dentin CTE of 1.0×10^{-5} K^{-1} for alveolar bone and 1.14×10^{-5} K^{-1} for dentin. Further exploration in the open literature yields 1.14×10^{-5} K^{-1} for dentin by Lee et al.[17] Since the compositions and the microstructural-configuration of dentin are very much alike those of bone,[18] dentin CTE of 1.0×10^{-5} K^{-1} is thus used for the bone CTE in the present study.

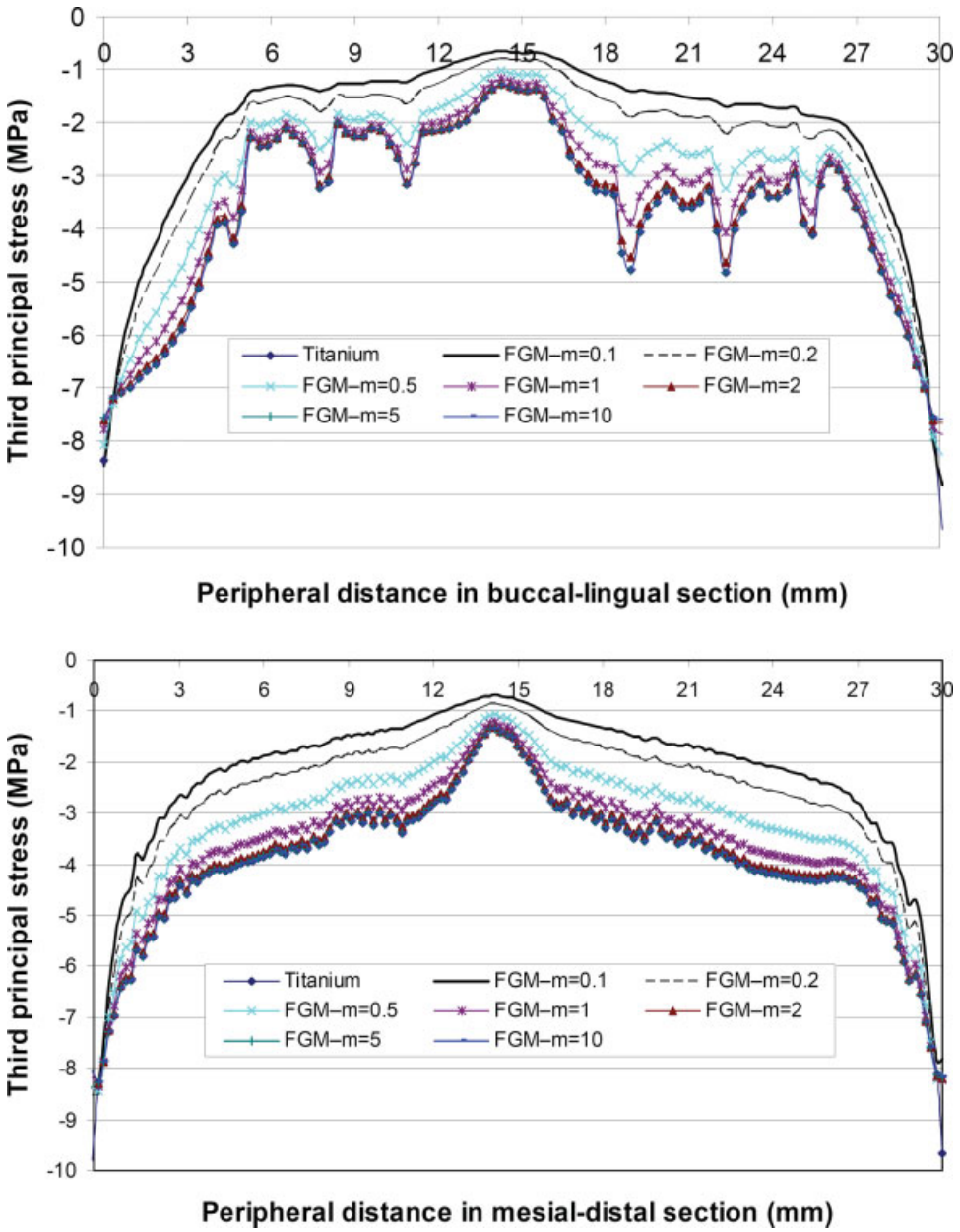

Figure 8. Peri-implant third principal stress under occlusal force only. [Color figure can be viewed in the online issue, which is available at www.interscience.wiley.com.]

For the FG dental implant, different mixture of exponential law along the length of implant is applied for the present parametric study. The exponential distributions is chosen simply because the volume fraction of the HA component will give one at the apex and zero at the connection with the abutment. In this way, there are not stress jumps at these places and yield the desirable highest biocompatibility at the apex. The volume fraction for the hydroxyapatite, V_h, is expressed as follows,

$$V_h = \left(\frac{H-z}{H}\right)^m \tag{1}$$

where z and H are the vertical position and the length of the dental implant. And the volume fraction for the titanium V_t is then written as

$$V_t = 1 - V_h. \tag{2}$$

The exponential index m in Eq. (1) is assigned different values from 0.1 to 10 to implement the parametric study. The volumetric fraction variation along the length of the dental implant with regard to different values of m is graphically shown in Figure 2.

The properties for the FG implant, i.e. the Young's modulus E, the Poisson's ratio υ, and the coefficients of the thermal expression C, are derived from the

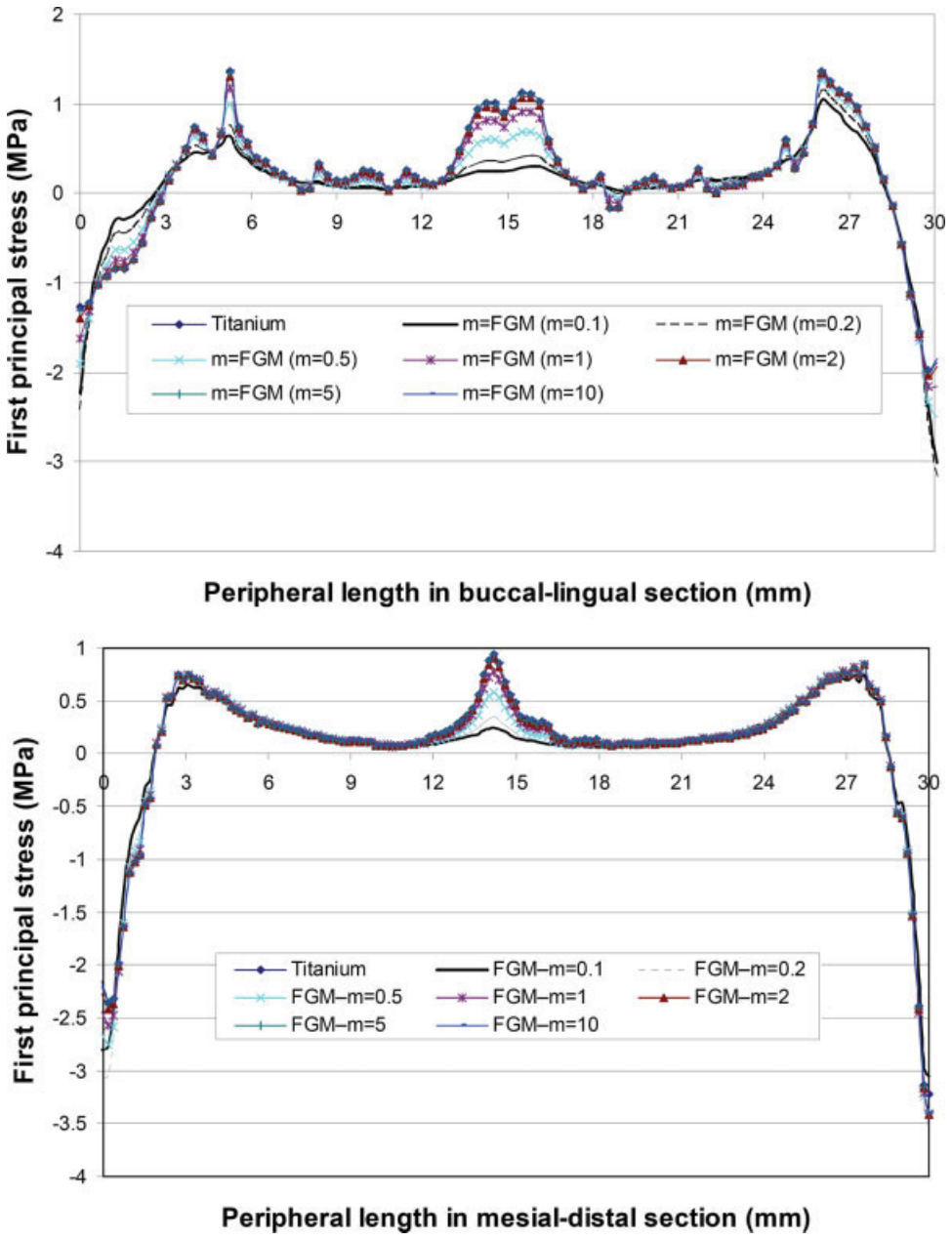

Figure 9. Peri-implant first principal shear stress under occlusal force only. [Color figure can be viewed in the online issue, which is available at www.interscience.wiley.com.]

properties of component hydroxyapatite (HA) and titanium levied by the respective volumetric fraction as follows,[12]

$$E = \frac{E_h\left\{E_h + (E_t - E_h)\, V_t^{2/3}\right\}}{E_h + (E_t - E_h)\left(V_t^{2/3} - V_t\right)} \tag{3}$$

$$v = v_t V_t + v_h V_h \tag{4}$$

$$C = \frac{C_t K_t V_t + C_h K_h V_h}{K_t V_t + K_h V_h} \tag{5}$$

$$K_t = \frac{E_t}{2(1 - v_t)}, \quad K_h = \frac{E_h}{2(1 - v_h)} \tag{6}$$

where subscript t and h stand for titanium and hydroxyapatite, respectively. The calculated variable Young's modulus and the coefficient of thermal expansion with regard to different exponential index m are plotted in Figure 3.

The discrete size of the mesh is 0.3 mm. A mesh size sensitivity analysis is carried out. The mesh with discrete size of 1, 0.5, and 0.3 mm, respectively, are applied for the dental implant and the immediate surrounding bone tissue. It is found that the meshes with 0.5 and 0.3 mm discrete size yield almost identical results, and

TABLE II
Maximum von Mises and Principal Stresses Along the Peripheries in Buccal–Lingual and Mesial-Distal Sections

Simulation Cases		von Mises Stress		Third Principal Stress		First Principal Stress	
		Maximum (MPa)	Location	Maximum (MPa)	Location	Maximum (MPa)	Location
$m = 0.1$	$\Delta T = -20°C$	7.6	Buc-cer	−9.31	Lin-cer	4.11	Dis-cer
	$\Delta T = 0°C$	5.86	Buc-cer	−8.82	Lin-cer	1.04	Lin-cer
	$\Delta T = 20°C$	6.65	Mes-cer	−10.70	Mes-cer	0.57	Lin-cer
$m = 0.2$	$\Delta T = -20°C$	7.61	Buc-cer	−9.25	Les-cer	3.93	Dis-cer
	$\Delta T = 0°C$	5.7	Buc-cer	−8.81	Lin-cer	1.14	Lin-cer
	$\Delta T = 20°C$	7.28	Mes-cer	−11.23	Mes-cer	0.92	Lin-cer
$m = 0.5$	$\Delta T = -20°C$	8.62	Lin-cer	−8.60	Lin-cer	4.41	Mes-cer
	$\Delta T = 0°C$	5.84	Buc-cer	−8.45	Mes-cer	1.26	Lin-cer
	$\Delta T = 20°C$	6.68	Dis-cer	−12.98	Dis-cer	1.31	Dis-cer
$m = 1$	$\Delta T = -20°C$	9.15	Lin-cer	−8.10	Lin-cer	4.67	Dis-cer
	$\Delta T = 0°C$	5.82	Buc-cer	−8.36	Mes-cer	1.32	Lin-cer
	$\Delta T = 20°C$	6.98	Dis-cer	−12.03	Dis-cer	1.26	Dis-cer
$m = 2$	$\Delta T = -20°C$	9.76	Lin-cer	−8.27	Lin-cer	5.15	Dis-cer
	$\Delta T = 0°C$	5.86	Mes-cer	−8.30	Mes-cer	1.31	Buc-mid
	$\Delta T = 20°C$	6.03	Dis-cer	−13.45	Dis-cer	1.21	Dis-cer
$m = 5$	$\Delta T = -20°C$	9.5	Dis-cer	−12.89	Dis-cer	1.38	Dis-mid
	$\Delta T = 0°C$	5.89	Mes-cer	−8.28	Mes-cer	1.36	Buc-mid
	$\Delta T = 20°C$	7.07	Lin-cer	−7.68	Lin-cer	4.83	Dis-cer
$m = 10$	$\Delta T = -20°C$	9.51	Buc-cer	−12.90	Lin-cer	1.38	Dis-cer
	$\Delta T = 0°C$	5.89	Buc-cer	−8.28	Mes-cer	1.36	Lin-cer
	$\Delta T = 20°C$	7.07	Mes-cer	−7.70	Lin-cer	4.84	Dis-cer
Titanium	$\Delta T = -20°C$	9.45	Buc-cer	−15.18	Buc-cer	1.39	Mes-cer
	$\Delta T = 0°C$	8.02	Mes-cer	−8.69	Dis-cer	1.39	Buc-cer
	$\Delta T = 20°C$	9.41	Mes-cer	−8.68	Mes-cer	4.83	Buc-mid

Buc-cer, buccle-cervical; Dis-cer, distal-cervical; Lin-cer, lingual-cervical; Mes-cer, mesial-cervical; Lin-mid, lingual-middle; Buc-mid, bucccal-middle.

the maximum von Mises stress derived with the mesh of 0.5 mm discrete size has a discrepancy of 0.2% to that with 0.3 mm discrete size. On the other hand, the mesh with 1 mm discrete size has substantial difference in terms of von Mises stress to those from meshes with 0.3 and 0.5 mm discrete sizes. Thus, the current study adopts the mesh with a discrete size of 0.3 mm. Coarser mesh is used for the bone tissue that is far away from the implant. Totally, 199,008 tetragonal elements and 35,143 nodes are included in the model.

A user-subroutine UFIELD in Abaqus is used to implement the FG material properties of the implant. The smooth material properties variation of the dental implant is replaced by segmented lines, such as the CTE approximation as shown in Figure 4. Currently, one-thousand segments are adopted to represent the actual material property variation. With reference to the total length of dental implant of 13 mm, the segment length of 0.013 mm is much smaller than the mesh size of 0.3 mm. Thus, the present simulation of FG material can achieve the maximum accuracy of the FE method for homogeneous materials.

THE FE MODEL VERIFICATION

The original titanium material properties used in Las Casas et al.'s[14] simulation is implemented by the Abaqus user-subroutine, in which the variation of the material properties is replaced by the constant material data of titanium. Only the occlusal force of 100*N* is applied. The first principal and third principal stresses along the peripheries of the buccal–lingual and mesial–distal sections are compared in Figure 5. It can be seen from Figure 5 that the current simulation results generally approach the simulation results by Las Casas et al.[14] in terms of the overall stress levels and the trends. The differences between the peak values may result from the different meshes and sampling nodal positions. The current simulation uses more refined mesh than that of Las Casas et al.,[14] so the stress curves are much smoother than those of Las Casas et al.[14]

The peripheral nodes used to show the stresses in Figure 5 and all the following figures are plotted in Figure 6. And the shape of the tapered cutting is highlighted in Figure 6.

SIMULATION RESULTS

Figures 7–9 give the peri-implant von Mises, first principal/tensile and third principal/compressive stresses under occlusal force only for different FG and the titanium implants, respectively. The legends

for the curves are self-explained, e.g., FGM-$m = 0.1$ represents the implant of FG material with the HA fraction exponential index of $m = 0.1$. The different FG implant gives very similar variation patterns of peri-implant stresses. In view of the general stress level, the FG implant with the smallest HA fraction exponential index ($m = 0.1$) defines the lower bound, while the titanium implant registers the upper bound. Basically, the ascending order follows the exponential index increasing order, i.e. the higher the exponential index, the higher the overall stresses. It conforms to the Young's modulus variation tendency as shown in Figure 3 that the higher the exponential index, the higher the overall Young's modulus. The reason is that the implant and the surrounding bone could be assumed as two parallel springs to balance the occlusal force, the higher the stiffness of implant, the higher share of forces it takes. It is worth mentioning that in the Figures 7–9, the peak stresses in the buccal–lingual sections are caused by the three pairs of the tapered cuttings.

It should be noted that the lower negative algebraic value in Figure 8 stands for higher compressive stress. The maximum values along the peripheries are listed in Table II for all the simulation cases, and the histogram plot in Figure 10 shows those for all the implants under occlusal force only. Almost all of the maximum stress values locate at the cervical area with very few exceptions. The highest von Mises stress (8.02 MPa) comes from the titanium implant, which is 40.7% higher than the lowest counterpart from FG implant with $m = 0.2$ (5.7 MPa).

The differences in the maximum third principal/compressive and the first principal/tensile stresses are not so prominent as it is for the maximum von Mises stresses. The highest third principal/compressive stress comes from the FG implant with $m = 0.1$ (−8.82 MPa), which is only 6.5% higher than that of the lowest value from FG implant of $m = 2$ (−8.28 MPa). The maximum tensile stress comes from titanium implant (1.39 MPa), which is 33.6% higher than the lowest value from FG implant with $m = 0.1$ (1.04 MPa). Although the percentage difference for the tensile stress is high, the absolute difference is still very small since the maximum tensile stresses for all the implants are much smaller than the compressive counterparts.

Very minor differences are found for all the maximum stresses among the FG implants. The FG implants with $m = 0.1$, 5, 10 give the highest von Mises stress (5.89 MPa), while the FG implant with $m = 0.2$ gives the lowest (5.7 MPa). The highest maximum third principal stress for all the FG implants comes from that with $m = 0.1$ (−8.82 MPa), while the lowest from both the FG implants with $m = 5$ and 10 (−8.28 MPa). The highest maximum first principal stress comes from the FG implants with $m = 5$ and 10 (1.36 MPa), the lowest comes from FG implant with $m = 0.1$ (1.04 MPa). The percentage difference between the highest and lowest are 3.33, 6.52, and 30.76% of the lowest maximum values for the von Mises, compressive and tensile stresses, respectively. Although the percentage difference for the maximum tensile stress is as high as 30.76%, the absolute difference value is very small since the tensile stress is generally very low. Thus, it can be stated that under occlusal force only, the mechanical performance of all the FG implants are almost equally good, while the titanium sustains much higher maximum von Mises stresses.

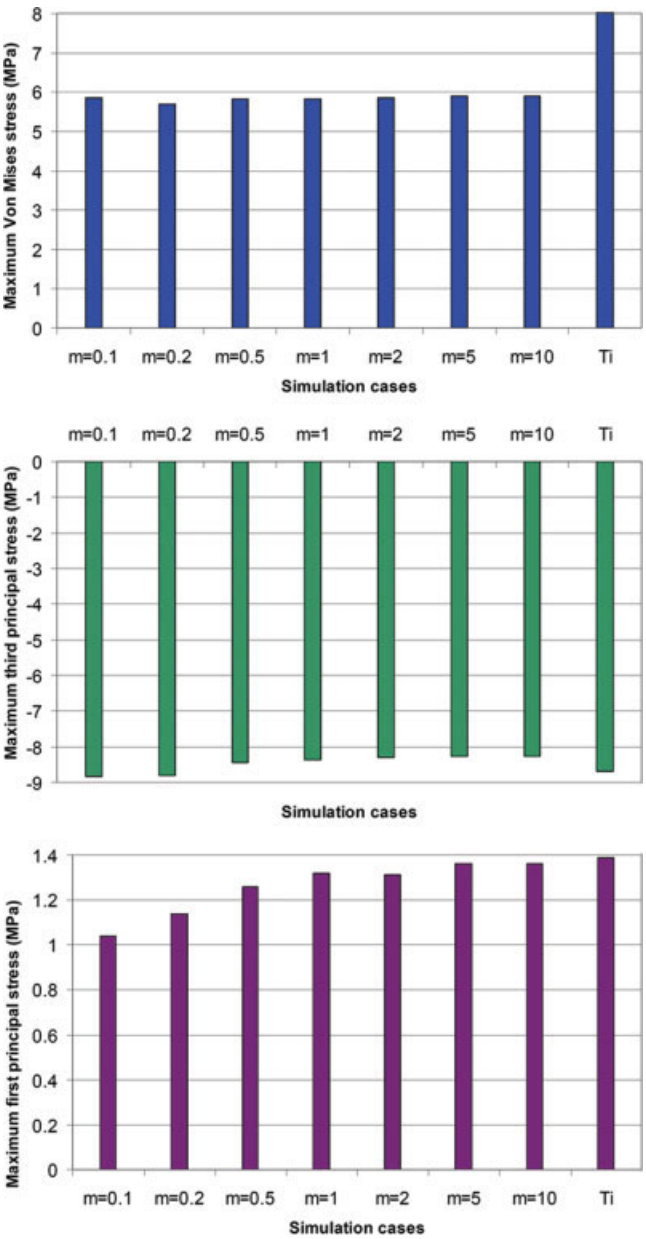

Figure 10. Maximum peri-implant stresses in buccal–lingual and mesial–distal sections under occlusal force only. [Color figure can be viewed in the online issue, which is available at www.interscience.wiley.com.]

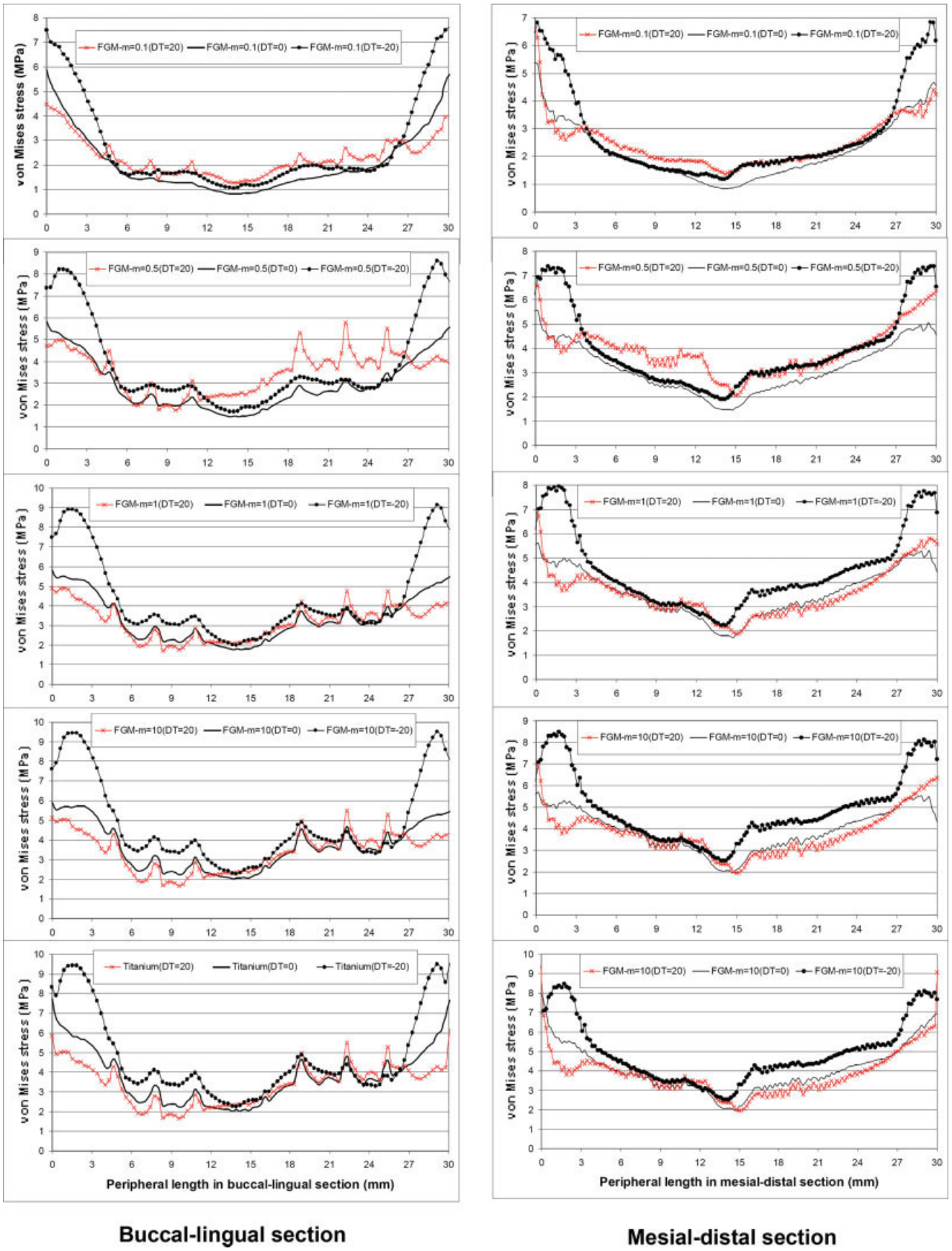

Figure 11. Temperature effect on peri-implant von Mises stress. [Color figure can be viewed in the online issue, which is available at www.interscience.wiley.com.]

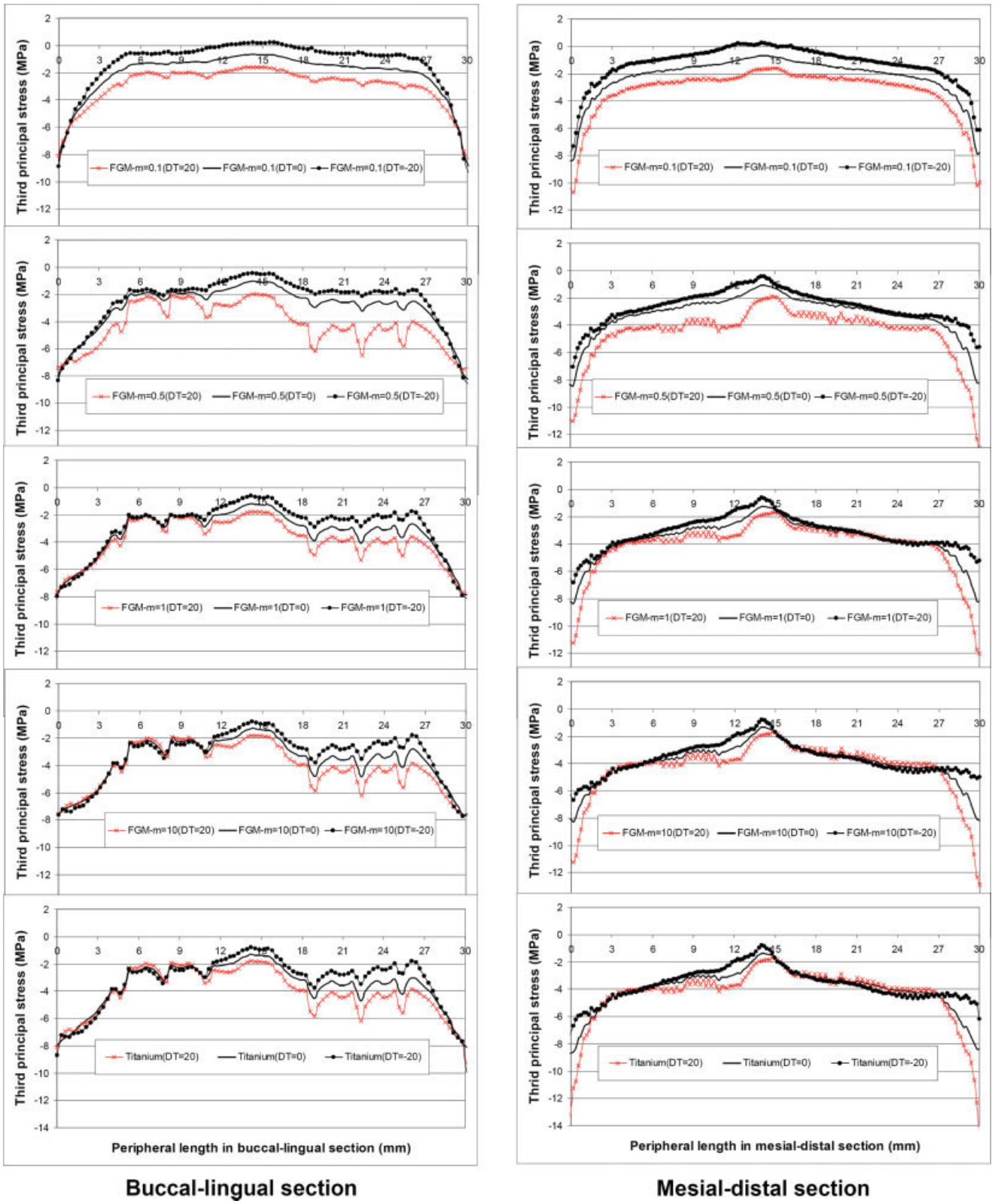

Figure 12. Temperature effect on peri-implant third principal stress. [Color figure can be viewed in the online issue, which is available at www.interscience.wiley.com.]

The effect of temperature change due to daily oral activity is demonstrated from the simulations of −20 and 20°C temperature loads applied besides the occlusal force. The peri-implant stresses for four selected FG and titanium implants are shown in Figures 11–13. It can be seen from these figures that the

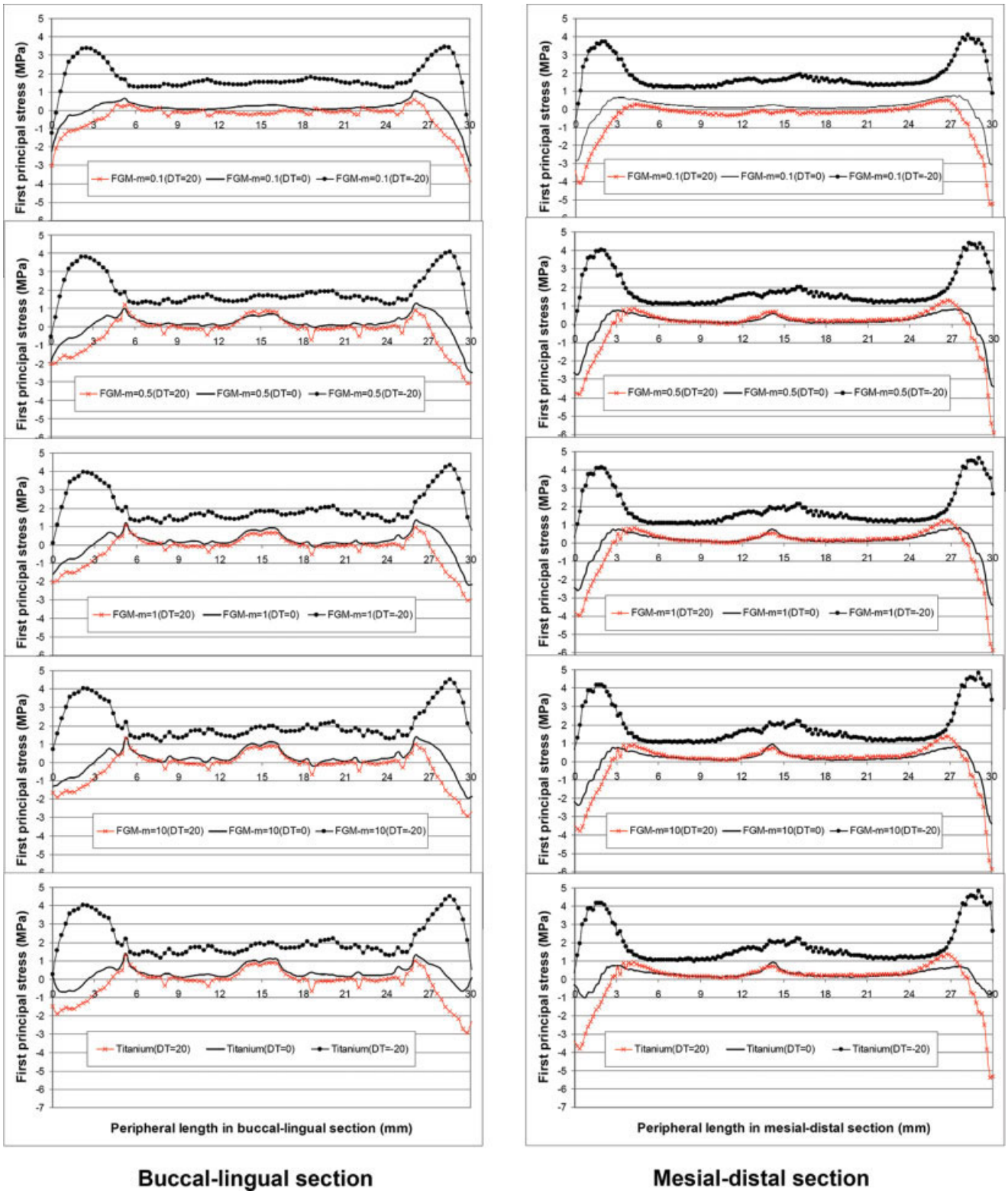

Figure 13. Temperature effect on peri-implant first principal shear stress. [Color figure can be viewed in the online issue, which is available at www.interscience.wiley.com.]

temperature change has more remarkable effect on the cervical area than on the other areas.

The effect of temperature change on the von Mises stress is shown in Figure 11. It is seen that reduction of temperature increases the stress level remarkably, while the temperature increase lowers it slightly. It should be mentioned that the DT in the legends stands for the temperature load, e.g. DT = 0°C indi-

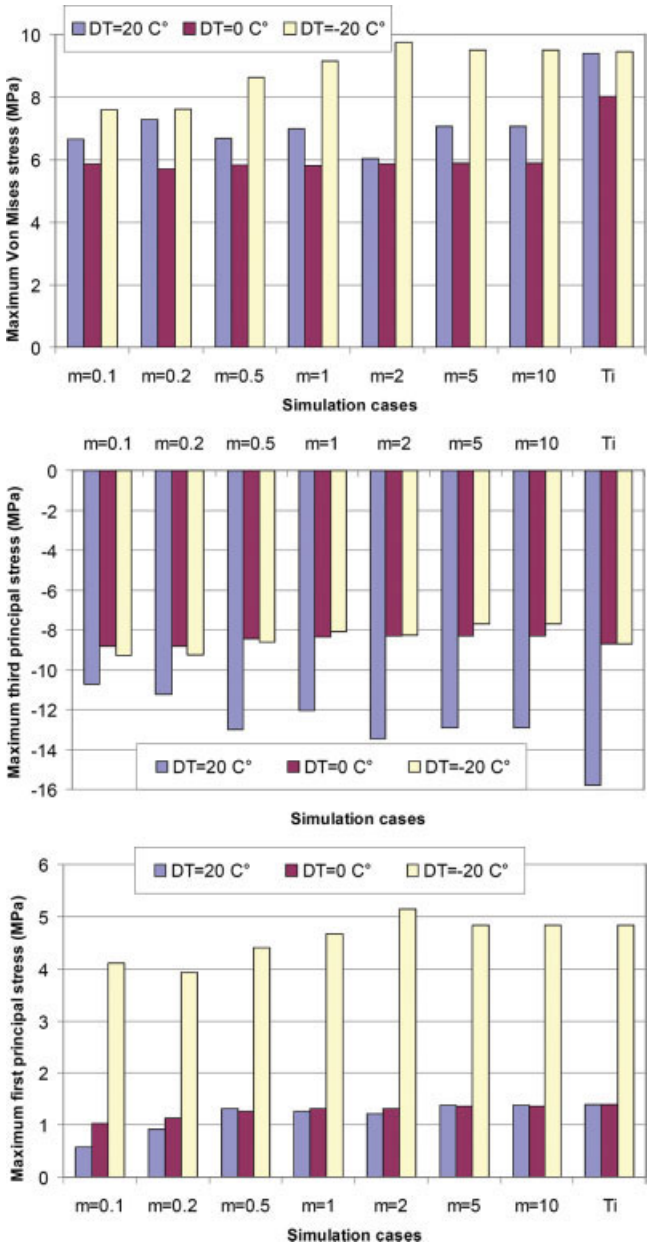

Figure 14. Maximum peri-implant stresses in buccal–lingual and mesial–distal sections under both occlusal and temperature loads. [Color figure can be viewed in the online issue, which is available at www.interscience.wiley.com.]

cates a zero temperature–load case and DT = 20°C means that the temperature load is 20°C.

For the compressive stress (Fig. 12), a temperature increment of 20°C increases the compressive stress more significantly than the similar temperature decrease reducing it. The effect is more remarkable on the cervical area in the mesial–distal section.

For the first principal stress, it can be seen from Figure 13 that, in spite of the different FG implants, the temperature load of −20°C/20°C increases/decreases the first principal stresses at the cervical area remarkably, while it does slightly at the apex area. And the effect is even more prominent at the cervical area in the mesial–distal section.

The temperature change effect is also reflected in Figure 14, which compares the maximum values in the peripheries of the buccal–lingual and the mesial–distal sections. It can be noted in Figure 14 and Table II that the FG implant with $m = 2$ sustains the highest maximum von Mises and first principal stresses with temperature decrease of 20°C (5.15 and 9.76 MPa, respectively) among all the implants. The highest maximum third principal stress comes from the titanium implant with a temperature decrease of 20°C (−15.18 MPa). The FG implant of $m = 2$ with a temperature decrease of 20°C (−13.45 MPa) also yields the highest third principal/compressive stress among the FG implants.

The FG implant with $m = 0.2$ without temperature load gives rise to the lowest maximum von Mises stress (5.7 MPa). The FG implant of $m = 10$ with temperature reduction of 20°C (−7.70 MPa) gives the minimum third principal stress. And FG implant of $m = 0.1$ with temperature decrease of 20°C gives the lowest maximum first principal stress (0.57 MPa).

In summary, decrease of temperature increases the stresses, especially the tensile stress remarkably. Relative mechanical performances of the FG and titanium implants under both the temperature load and the occlusal force are very different from those under occlusal force only.

With reference to the bending strength of 159 MPa of the implant-bone-bond,[8] it seems that the current derivation of the maximum tensile stress (15.18 MPa) for all the FG and titanium implants as seen in Table II would not cause any implant-bone-bond failure. However, the FG implant with $m = 2$ sustains the highest likelihood to implant-bone-bond failure amongst the FG dental implants because of repetitions or fatigue failure.

CONCLUSIONS

Under the occlusal force only, the FG implants with different HA fraction perform almost equally well, while the titanium yields much higher von Mises stress. Mismatch of coefficient of thermal expansion between the implant and the hosting bone causes additional stress when oral temperature is changed. It is derived from the current study that temperature decrease instead of increase changes the maximum stresses remarkably. It could triple the maximum tensile stress. The performance of dental implant in view of thermal stress is very different from that under occlusal force only. When temperature change effect is considered, the FG implant with HA fraction exponential index $m = 2$ sustains the

highest von Mises and tensile stresses among all the FG and titanium implants. Thus, thermal stress should not be ignored for evaluating the performance of dental implants.

The authors express their sincere appreciation and gratitude to Prof E. B. Las Casas from Escola de Engenharia, Universidade Federal de Minas Ferais, Brazil, for providing the dental implant model. From which, the authors obtain the geometry for the current FE model.

References

1. Noort RV. Introduction to Dental Materials, 2nd ed. London: Elsevier; 2002.
2. Roy ME, Rho JY, Tsui TY, Evans ND, Pharr GM. Mechanical and morphological variation of the human lumbar vertebral cortical and trabecular bone. J Biomed Mater Res 1999;44: 191–197.
3. Yang CY, Lin RM, Wang BC, Lee TM, Chang E, Hang YS, Chen PQ. In vitro and in vivo mechanical evaluations of plasma-sprayed hydroxyapatite coatings on titanium implants: The effect of coating characteristics. J Biomed Mater Res 1997; 37:335–345.
4. Svehla M, Morberg P, Zicat B, Bruce W, Sonnabend D, Walsh WR. Morphometric and mechanical evaluation of titanium implant integration: Comparison of five surface structures. J Biomed Mater Res 2000;51:15–22.
5. Cofino B, Fogarassy P, Millet P, Lodini A. Thermal residual stresses near the interface between plasma-sprayed hydroxyapatite coating and titanium substrate: Finite element analysis and synchrotron radiation measurements. J Biomed Mater Res A 2004;70:20–27.
6. Watari F, Yokoyama A, Saso F, Uo M, Kawasaki T. Fabrication and properties of functionally graded dental implant. Compos B Eng 1997;28:5–11.
7. Yokoyama A, Watari F, Miyao R, Matsuno H, Uo M, Kawasaki T, Kohgo T, Omori M, Hirai T. Mechanical properties and biocompatibility of titanium-hydroxyapatite implant material prepared by spark plasma sintering method. Key Eng Mater 2000;192/5:445–448.
8. Chu CL, Wang SD, Lin PH, Yin ZD, Zhu JC. Characterization and optimized design of HA-Ti/Ti/Ha-Ti symmetrical functionally graded biomaterial. Mat Sci Eng A 2001;316(1/2): 205–210.
9. Zhu JC, Chu CL, Yin ZD. Bonding strength of hydroxyapatite/Ti FGM implant to bone. Rare Met Mater Eng 2003;32: 432–435.
10. Chu CL, Zhu JC, Yin ZD, Lin PH. Optimal design and fabrication of hydroxyapatite-Ti asymmetrical functionally graded biomaterial. Mater Sci Eng A 2003;348(1/2):244–250.
11. Hedia HS, Mahmoud NA. Design optimization of functionally graded dental implant. Biomed Mater Eng 2004;14:133–143.
12. Takashi F, Naotake N. Analysis of thermal stress in a plate of functionally gradient material. JSAE Rev 1995;16:263–268.
13. Toparli M, Sasaki S. Finite element analysis of the temperature and thermal stress in a postrestored tooth. J Oral Rehabil 2003;30:921–926.
14. Las Casas EB, Cimini JCA, Cornacchia TPM, Lanza M, Vieira AC. Numerical simulations in dental mechanics and orthodontics: Some examples of applications. In: Las Casas EB, Pamplona DC, editor. Computational Models in Biomechanics. Barcelona: CIMNE; 2004, p 103–139.
15. Ahmed AM, Nair R, Burke DL, Miller J. Transient and residual stresses and displacements in self-curing bone cement, Part 2: Thermoelastic analysis of the stem fixation system. J Biomech Eng 1982;104:28–37.
16. Duck RA. Physical Properties of Tissue: A Comprehensive Reference Book.Academic Press: San Diego, CA; 1990.
17. Lee SY, Chiang HC, Huang HM, Shih YH, Chen HC, Dong DR, Lin CT. Thermo-debonding mechanisms in dentin bonding systems using finite element analysis. Biomaterials 2001; 22:113–123.
18. Currey JD.The structure of bone tissue. Available at: www.loc.gov/catdir/samples/prin031/2001043148.html.